Human Activity Recognition Using Deep Learning Networks with Enhanced Channel State information

Zhenguo Shi, J. Andrew Zhang, Richard Xu, and Gengfa Fang
Global Big Data Technologies Center
University of Technology Sydney, Sydney, Australia
{Zhenguo.Shi; Andrew.Zhang; Yida.Xu; gengfa.fang}@uts.edu.au

Abstract—**Channel State Information (CSI) is widely used for device free human activity recognition. Feature extraction remains as one of the most challenging tasks in a dynamic and complex environment. In this paper, we propose a human activity recognition scheme using Deep Learning Networks with enhanced Channel State information (DLN-eCSI). We develop a CSI feature enhancement scheme (CFES), including two modules of background reduction and correlation feature enhancement, for preprocessing the data input to the DLN. After cleaning and compressing the signals using CFES, we apply the recurrent neural networking (RNN) to automatically extract deeper features and then the softmax regression algorithm for activity classification. Extensive experiments are conducted to validate the effectiveness of the proposed scheme.**

Index Terms—**human activity recognition, WiFi, device free sensing, deep learning, channel state information.**

I. INTRODUCTION

Device-free human activity recognition (DF-HAR) using wireless signals are attracting significant research interests [1]. Compared with conventional device-based sensing techniques (e.g., wearable devices), DF-HAR does not require the targeting users to wear any devices. Moreover, DF-HAR is able to complete the sensing task without exposing user's private information, such as the face of user. In the context of DF-HAR, WiFi-based HAR is receiving particular attention because of its wide availability [2].

Existing WiFi-based HAR techniques can be categorized into two main branches: leveraging the received signal strength (RSS) of WiFi signals [3], [4] and the channel state information (CSI) of WiFi physical layer information [5]. The RSS-based human activity recognition (RSS-HAS) can achieve a fair sensing accuracy by utilizing the variations of RSS, e.g., means, peak-to-peak values of RSS, etc. However, it is vulnerable to the shadow fading and the multi-path effect, and the sensing accuracy will degrade severely if the environment is complex [6]. The CSI-based human activity recognition (CSI-HAS) uses the CSI that represents more fine-grained information, and is more promising for achieving better recognition performance. A lot of existing work on CSI-HAS devotes to improving the sensing accuracy by leveraging signal processing measurements. For example, the principal component analysis (PCA) [7] and discrete wavelet transform (DWT) [8] are applied to remove background noise and improve the quality of CSI. However, these methods often face challenges such as feature selections and feature fusions, which can degrade the sensing performance severely.

To solve these problems, Deep learning networks (DLN) is used to extract and transform the inherent features automatically from the input data for CSI-HAS [9], [10], [11]. In [9], a sparse auto-encoder (SAE) network is used as a feature optimizer, but its sensing performance is susceptible to the quality of input features. In [11], long-short term memory (LSTM) based recurrent neural networking (LSTM-RNN) is applied, using the raw CSI as the input. However, training the RNN is time-consuming due to the large amount of raw CSI packets.

In this paper, we propose a HAR scheme using Deep Learning Networks with enhanced CSI (DLN-eCSI), which can achieve significantly improved sensing performance with reduced training complexity. We develop a CSI feature enhancement scheme (CFES) for cleaning and compressing signals input to the DLN. CFES includes two modules: background reduction and correlation feature enhancement. In background reduction, we propose two methods for removing activity-unrelated information from CSI. In correlation feature enhancement, we compute correlation signals over all subcarriers and streams to improve the reliability of feature signals, as well as compressing the signals. We then use LSTM-RNN to extract the deeper features from the enhanced correlation signals. Extensive experiments are conducted and the results demonstrate that the proposed DLN-eCSI scheme achieves much better sensing accuracy, with significantly reduced complexity, compared with conventional CSI-based RNN sensing methods.

The rest of this paper is organized below. Section II reviews the system model. The detailed methodology of the proposed scheme is presented in Section III. Section IV provides detailed experimental settings and the performance results. Section V concludes the paper.

II. SYSTEM MODEL

In this section, we introduce the system architecture for the proposed DLN-eCSI scheme, as shown in Fig. 1. DLN-eCSI aims to recognize human activities in three main stages: data collection, data processing, and deeper feature extraction and classification.

In the stage of data collection, from wireless communication links between the transmitters and receivers, the physical layer
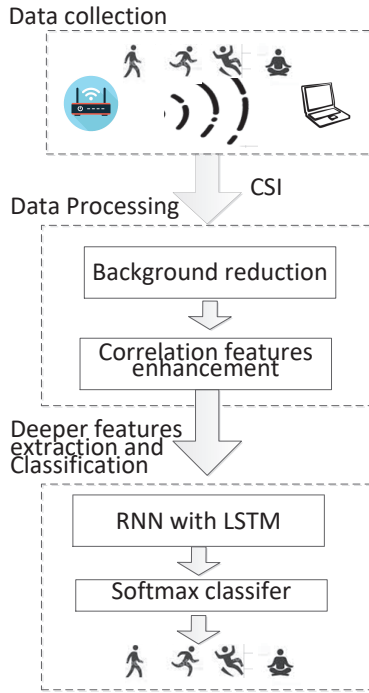
Fig. 1. A sketch of the human activity recognition system based on WiFi 802.11n
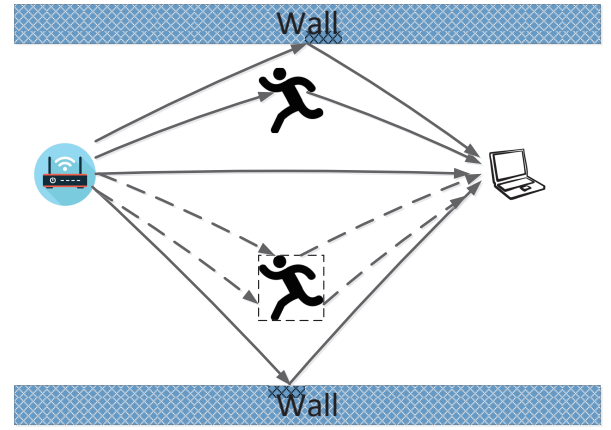

Fig. 2. Influence of human activity on signal propagation.

extractor, and the softmax regression algorithm [9] is adopted as the classifier. The deep learning network can be trained during the training process using the training data offline. Then during the online sensing phase, the proposed scheme classifies the human activities using the trained network coefficients.

III. METHODOLOGY

In this section, we present the process of the proposed DLN-eCSI in details.

A. Data collection

Let N_T and N_R stand for the number of antennas at the transmitter and receiver, respectively. Thus, there are $L = N_T \times N_R$ streams (links) contained in a CSI packet, which can be expressed as

$$\mathbf{H}(n) = [H^{1,1}(n),\ldots,H^{s,1}(n),\ldots,H^{s,l}(n),\ldots,H^{S,L}(n)]^T, \quad (1)$$

where $\mathbf{H}(n)$ represents the CSI vector obtained at time n, l is the indicator of the lth stream, S denotes the total number of available subcarriers in each stream, s denotes the sth subcarrier in the stream, and T stands for the transposition operation. Then the CSI matrix within a time period (e.g., $n = 1, 2, \ldots, N$) is adopted to sense the human activities, and is given by

$$\mathbf{H} = [\mathbf{H}(1), \ldots, \mathbf{H}(n) \ldots, \mathbf{H}(N)]. \quad (2)$$

B. Data Processing

Note that the CSI matrix $\mathbf{H}$ in (2) is only the raw information, which is not suitable for HAR directly for the following reasons. First, $\mathbf{H}$ contains too much activity-unrelated information, which will degrade the quality of extracted features. Second, applying $\mathbf{H}$ directly to detect human activities (such as in [11]) is time-consuming and increases the system overhead due to the large size of $\mathbf{H}$. We use CFES, including background reduction and correlation feature enhancement modules, to overcome these problems.

information (e.g., CSI), which reflects the variations of the wireless environment caused by human activities, is collected for processing at the receivers. When a person performs certain activities such as running in an indoor environment covered by a wireless network, the wireless signal propagation is distorted with changes in both the number of multipath signals and their amplitudes and phases. These distortions will cause the variation of CSI. The receivers are typically WiFi access points in our considered setup. In this paper, we use the widely adopted Intel 5300 802.11n network interface card for CSI acquisition [12]. The CSI at 30 subcarriers from all three antennas is used. More details are provided in Section IV-A.

In the stage of data processing, activity-unrelated information is removed and unique features are extracted from CSI for detecting human activities. In this stage, we use the proposed CFES for *background reduction* and *correlation feature enhancement*. The background reduction module is used to filter out activity-unrelated components in the raw CSI and obtain enhanced CSI with information ideally solely related to human activities. The correlation feature enhancement module is applied to extract unique correlation features from the enhanced CSI at the OFDM subcarrier level. In this stage, all the subcarriers are employed to calculate the correlation feature matrix which will be used for identifying distinctive feature patterns of different activities.

In the last stage of deeper feature extraction and classification, the deeper features are automatically extracted from the output in the previous stage. To that end, a deep learning network (e.g., LSTM-RNN) is employed as the features

1) Background reduction: The core task in the background reduction module is to filter out the activity-unrelated information while retaining the activity-related information. Although human activities may cause the distortion of some multipath signals, there could generally be more multipath largely unchanged. Thus $\mathbf{H}$ can be divided into two parts: dynamic CSI and static CSI, which can be expressed as

$$\mathbf{H}(n) = \mathbf{H}_{dy}(n) + \mathbf{H}_{st}(n), \tag{3}$$

where $\mathbf{H}_{dy}(n)$ represents the vector of dynamic CSI affected by the movement of human. $\mathbf{H}_{st}(n)$ stands for the static CSI vector which is largely unchanged. Note that the impact of $\mathbf{H}_{st}(n)$ on $\mathbf{H}(n)$ is usually greater than $\mathbf{H}_{dy}(n)$, because the influence of human activities on the whole environment is generally limited, especially when a person performs minor actions such as standing, sitting and raising hands, etc. The sensing accuracy would degrade severely if $\mathbf{H}(n)$ is directly utilized for detecting human activities. Therefore, it is much desirable to remove the static information $\mathbf{H}_{st}(n)$ from $\mathbf{H}(n)$. Next we propose two methods for mitigating $\mathbf{H}_{st}(n)$ from $\mathbf{H}(n)$.

We call the first one as the *local mean (LM)* method which estimates $\mathbf{H}_{st}(n)$ over a period of time using the exponentially weighted moving average (EWMA) approach [13]. The estimated value of $\mathbf{H}_{st}(n)$ is

$$\widehat{\mathbf{H}}_{st}(n) = \alpha \mathbf{H}(n) + (1-\alpha)\widehat{\mathbf{H}}_{st}(n-1), \tag{4}$$

where $\widehat{\mathbf{H}}_{st}(n)$ denotes the estimated static CSI, and α represents the forgetting factor. The initial value of $\widehat{\mathbf{H}}_{st}(1)$ is set as $\mathbf{H}(1)$. Then the estimated dynamic CSI, $\widehat{\mathbf{H}}_{dy}(n)$, is equal to

$$\widehat{\mathbf{H}}_{dy}(n) = \mathbf{H}(n) - \widehat{\mathbf{H}}_{st}(n). \tag{5}$$

Thus, the whole estimated dynamic CSI matrix is

$$\widehat{\mathbf{H}}_{dy} = [\widehat{\mathbf{H}}_{dy}(1), \ldots, \widehat{\mathbf{H}}_{dy}(n), \ldots, \widehat{\mathbf{H}}_{dy}(N)], \tag{6}$$

where $\widehat{\mathbf{H}}_{dy}(n)$ is defined as

$$\widehat{\mathbf{H}}_{dy}(n) = [\widehat{H}_{dy}^{1,1}(n), \ldots, \widehat{H}_{dy}^{s,1}(n), \ldots, \widehat{H}_{dy}^{s,l}(n), \ldots, \widehat{H}_{dy}^{S,L}(n)]^T. \tag{7}$$

We call the second one as the *differential method (DM)*, which extracts dynamic CSI from $\mathbf{H}(n)$. The DM method computes the difference of $\mathbf{H}$ between two time slot and is simpler to implement. The estimated dynamic CSI vector using DM is expressed as

$$\widehat{\mathbf{H}}_{dy}^*(n) = \mathbf{H}(n) - \mathbf{H}(n-1), \tag{8}$$

where $\widehat{\mathbf{H}}_{dy}^*(n)$ denotes the estimated dynamic CSI, and $\widehat{\mathbf{H}}_{dy}^*(1) = \mathbf{0}$.

From (5) and (8), we can see that both LM and DM can extract the activity-related information contained in CSI. LM is capable of providing a high level of accuracy at the expense of relatively high complexity. The forgetting factor α affects the estimation performance, and its optimization is yet to be investigated. DM's computation complexity is lower, but with

sacrificed estimation performance. The impacts of LM and DM on the performance of human activity recognition will be provided in more details in Section IV.

2) Correlation Feature Enhancement: Let $\widehat{\mathbf{H}}_D$ denote the estimated dynamic CSI matrix hereafter, unless stated otherwise. The size of $\widehat{\mathbf{H}}_D$ is $SL \times N$ and will lead to high computational complexity if directly used for training and running in DLN. Here, we propose a novel method for significantly reducing the dimension of the input to DLN. This method is capable of extracting distinctive features from $\widehat{\mathbf{H}}_D$ and hence improving the recognition performance as well.

Different from existing methods which only leverage the correlation features of multiple subcarriers within one stream, e.g., [14], we compute the correlation between signals at all subcarriers from all streams, given by

$$\mathbf{C}_D = \widehat{\mathbf{H}}_D \times \widehat{\mathbf{H}}_D^T, \tag{9}$$

where $\mathbf{C}_D$ denotes the $SL \times SL$ correlation matrix. Such correlation information compresses the signals more effectively and provides more reliable features for behavior recognition. More specifically, the number of correlation features is significantly decreased from $SL \times N$ (i.e., the size of $\mathbf{H}_D$) to $SL \times SL$. The detailed performance assessment for CFES will be provided in Section IV.

C. Deeper Feature Extraction and Classification

In this section, we first extract the deeper features from $\mathbf{C}_D$ using LSTM-RNN, then classify human activities based on these extracted deeper features using the softmax regression algorithm. This process is demonstrated in Fig. 3.

The signal $\mathbf{C}_D$ contains compressed discriminative patterns for different human activities. We now feed it into LSTM-RNN to extract deeper features as shown in Fig. 3. The LSTM-RNN has the capability of extracting the deeper features of input data automatically. These extracted deeper features are then used to recognize human activities, through the softmax classifier. Note that the LSTM is able to distinguish similar behaviors, which can improve the recognition performance by distinguishing similar activities, such as "standing" and "stand up".

Conventional RNN-based sensing methods usually have a time-consuming training process, due to the large quantities of training data. By using overall correlation matrices with dramatically reduced volume of the input data, our DLN-eCSI scheme achieves significantly reduced training overhead.

IV. IMPLEMENTATION AND EVALUATION

In this section, we present the experimental results for evaluating the performance of the proposed DLN-eCSI scheme.

A. Experimental Setup

To evaluate the performance of the proposed DLN-eCSI, we conduct experiments in two indoor configurations, which are shown in Fig. 4. The first experimental environment is a $3m \times 4m$ office area where no obstacle is placed between the transmitter and receiver. The second one is a $4m \times 6m$
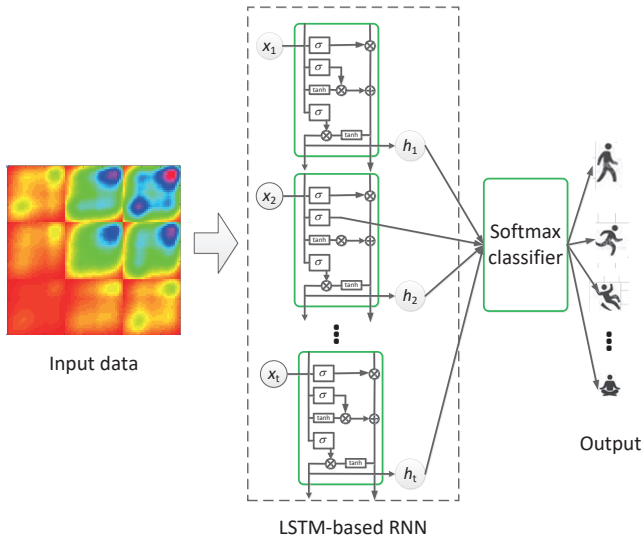
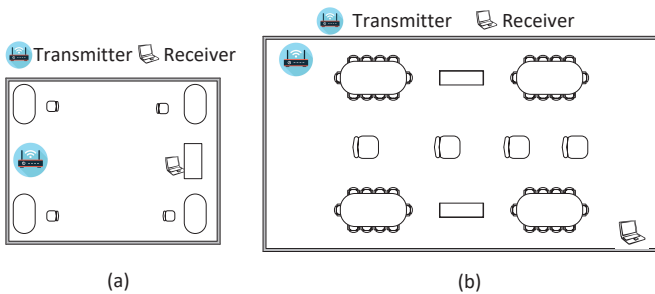Fig. 3. Structure of deeper features extraction and classification

Fig. 4. Layout of two experimental areas: (a) $3m \times 4m$ office. (b) $4m \times 6m$ laboratory.

laboratory where many tables are placed between the transmitter and receiver. Two computers equipped with Intel WiFi 5300 network card are used as the transmitter and receiver, respectively. The transmitter continues sending packets with one antenna ($N_T = 1$) at 2.4GHz frequency band based on the protocol of IEEE 802.11n. Using the CSI tools [12], the receiver equipped with 3 antennas ($N_R = 3$) obtains and records CSI for 30 subcarriers ($S = 30$). A person performs six different activities and repeats each activity for 400 times in each experimental environment. Each activity lasts for approximately 2s and the sample rate is 1KHz, thus the size of $\mathbf{H}$ is 90×2000. The LSTM-RNN applied in this paper has one hidden layer with 200 hidden units. The batch size and learning rate are set as 200 and 0.001, respectively.

B. Performance Evaluation

In this section, we evaluate the performance of our proposed DLN-eCSI by comparing it with other state-of-the-art methods. Various parameters and methods are used to provide a comprehensive comparison.

Fig. 5 compares the performance for two similar activities (i.e., sitting and sit down), using the original CSI matrix $\mathbf{H}$,

Experiment Methods	1st Exp.	2nd Exp.
RNN [11]	94.2%	89.8%
DLN-eCSI-L	97.5%	96.7%
DLN-eCSI-D	94.7%	92%

the estimated dynamic CSI $\widehat{\mathbf{H}}_D$ and the correlation feature matrix $\mathbf{C}_D$, respectively. As can be seen from Figs. 5(a) and 5(d), it is challenging to differentiate between "sitting" and "sit down" based on $\mathbf{H}$. However, they can be readily separated by using $\mathbf{C}_D$ as is clear from Figs. 5(c) and 5(f), because $\mathbf{C}_D$ significantly enhance the differences between these two activities. Moreover, the size of $\mathbf{C}_D$ (i.e., 90×90) is much smaller than $\mathbf{H}$ (i.e., 90×2000). Therefore, the training complexity is notably reduced in LSTM-RNN.

Table I shows the average sensing accuracy for LM and DM for six different activities. DLN-eCSI-L and DLN-eCSI-D are used to denote the cases when DLN-eCSI adopts LM and DM to extract the dynamic CSI, respectively. DLN-eCSI-L clearly outperforms the other two methods in both indoor configurations. Specifically, in the second configuration, the sensing accuracy of DLN-eCSI-L and DLN-eCSI-D are 96.7% and 92%, respectively. However, the sensing accuracy of RNN [11] is only 89.8%. In addition, for each method, the sensing accuracy in the first configuration is better than that in the second one, because the environment in the first configuration is simpler and hence it is easier for human activity recognition.

To further analyze the performance of different methods, we provide the confusion matrix for different activities in the second experimental configuration in Fig 6. DLN-eCSI-L achieves much higher sensing accuracy than the RNN method [11] for all the six activities, so does DLN-eCSI-D. For instance, the overall sensing accuracy of DLN-eCSI-L and DLN-eCSI-D for each activity is all above 0.869 and 0.831, respectively, but the accuracy for RNN is only 0.798.

Fig. 7 illustrates the impact of the number of subcarriers on the sensing accuracy of various methods in two configurations. Obviously, in both configurations, DLN-eCSI-L achieves the best sensing performance among these three methods increasing the number of subcarriers. For instance, when the number of subcarriers is 60, the sensing accuracy for DLN-eCSI-L and DLN-eCSI-D in the second configuration are 0.93 and 0.902, respectively. By contrast, the sensing accuracy for RNN in [11] is only 0.873. Notably, when the number of subcarriers is less than 60, the sensing accuracy of DLN-eCSI-D is lower than that of RNN in [11], while the training time in LSTM-RNN of DLN-eCSI-D is much smaller than RNN (refer to Table II).

Table II compares the training time of LSTM-RNN for various methods with different Hidden units. We utilize a 3.4GHz PC with Nvidia P4000 graphic card (8GB memory) to train the LSTM-RNN. The number of training iteration is
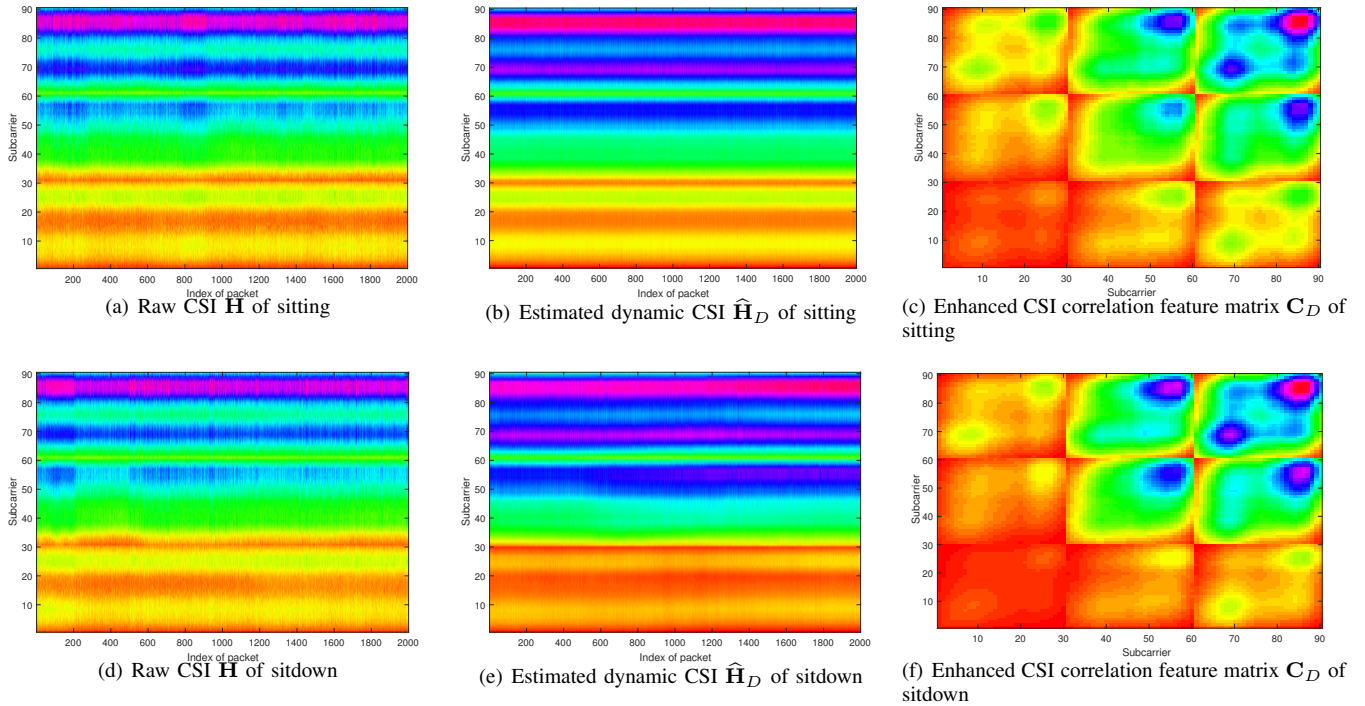
(a) Raw CSI $\mathbf{H}$ of sitting

(b) Estimated dynamic CSI $\widehat{\mathbf{H}}_D$ of sitting

(c) Enhanced CSI correlation feature matrix $\mathbf{C}_D$ of sitting

(d) Raw CSI $\mathbf{H}$ of sitdown

(e) Estimated dynamic CSI $\widehat{\mathbf{H}}_D$ of sitdown

(f) Enhanced CSI correlation feature matrix $\mathbf{C}_D$ of sitdown

Fig. 5. Performance of the proposed CSI feature enhancement scheme, when comparing two similar activities "sitting" and "sit down".

TABLE II
TRAINING TIME FOR DIFFERENT METHODS

Methods / Hidden units	50	200	400
RNN [11]	1773.8s	2848.6s	5107.2s
DLN-eCSI-L	283.7s	459.1s	1205.4s
DLN-eCSI-D	282.5s	458.2s	1203.3s

1000 and the training data set contains 1200 samples. It is clear that our proposed methods are superior to the RNN method in [11]. Specifically, when the number of hidden units is 400, the training time of LSTM-RNN for our proposed two methods are less than one-quarter of that for RNN in [11].

V. CONCLUSION

In this paper, we proposed a novel DLN-eCSI scheme for device free human activity recognition. We developed the CFES method for data preprocessing including background reduction and correlation feature enhancement. Two methods, the local mean and differential methods, are proposed to remove activity-unrelated information from the measured CSI. The correlation features of the activity-related information are enhanced via computing correlation over all subcarriers and streams, together with compressed data volume. We utilized LSTM-RNN network for detecting human activities by leveraging the enhanced features obtained from the CFES. We conducted a wide range of experiments, which demonstrate that the proposed scheme achieves significantly improved recognition accuracy, as well as notably reduced complexity.

REFERENCES

[1] X. Huang and M. Dai, "Indoor device-free activity recognition based on radio signal," *IEEE Transactions on Vehicular Technology*, vol. 66, no. 6, pp. 5316–5329, June 2017.

[2] D. Wu, D. Zhang, C. Xu, H. Wang, and X. Li, "Device-free wifi human sensing: From pattern-based to model-based approaches," *IEEE Communications Magazine*, vol. 55, no. 10, pp. 91–97, OCTOBER 2017.

[3] J. Wilson and N. Patwari, "Radio tomographic imaging with wireless networks," *IEEE Transactions on Mobile Computing*, vol. 9, no. 5, pp. 621–632, May 2010.

[4] S. Orphomma and N. Swangmuang, "Exploiting the wireless rf fading for human activity recognition," in *2013 10th International Conference on Electrical Engineering/Electronics, Computer, Telecommunications and Information Technology*, May 2013, pp. 1–5.

[5] J. Wang, L. Zhang, Q. Gao, M. Pan, and H. Wang, "Device-free wireless sensing in complex scenarios using spatial structural information," *IEEE Transactions on Wireless Communications*, vol. 17, no. 4, pp. 2432–2442, April 2018.

[6] S. Sigg, S. Shi, F. Buesching, Y. Ji, and L. Wolf, "Leveraging rf-channel fluctuation for activity recognition: Active and passive systems, continuous and rssi-based signal features," in *Proceedings of International Conference on Advances in Mobile Computing & Multimedia*, ser. MoMM '13. New York, NY, USA: ACM, 2013, pp. 43:43–43:52. [Online]. Available: http://doi.acm.org/10.1145/2536853.2536873

[7] W. Wang, A. X. Liu, M. Shahzad, K. Ling, and S. Lu, "Understanding and modeling of wifi signal based human activity recognition," in *Proceedings of the 21st Annual International Conference on Mobile Computing and Networking*, ser. MobiCom '15. New York, NY, USA: ACM, 2015, pp. 65–76. [Online]. Available: http://doi.acm.org/10.1145/2789168.2790093

[8] S. Zhong, Y. Huang, R. Ruby, L. Wang, Y. X. Qiu, and K. Wu, "Wi-fire: Device-free fire detection using wifi networks," in *2017 IEEE International Conference on Communications (ICC)*, May 2017, pp. 1–6.

[9] Q. Gao, J. Wang, X. Ma, X. Feng, and H. Wang, "Csi-based device-free wireless localization and activity recognition using radio image features," *IEEE Transactions on Vehicular Technology*, vol. 66, no. 11, pp. 10 346–10 356, Nov 2017.

Predicted activity

Actual activity	Stand up	Sitting	Walk	Standing	Sit down	Running
Stand up	0.869	0.006	0.019	0.106	0	0
Sitting	0.001	0.987	0	0.003	0.009	0
Walk	0.01	0.006	0.965	0	0	0.019
Standing	0.006	0	0.001	0.993	0	0
Sit down	0	0.012	0.001	0	0.987	0
Running	0	0	0.001	0	0	0.999

(a) Proposed DLN-eCSI-L

Predicted activity

Actual activity	Stand up	Sitting	Walk	Standing	Sit down	Running
Stand up	0.85	0	0.025	0.125	0	0
Sitting	0.002	0.831	0	0.015	0.152	0
Walk	0	0	0.993	0	0	0.007
Standing	0.041	0	0.001	0.956	0	0.002
Sit down	0	0.075	0	0.037	0.869	0.019
Running	0	0	0.006	0	0	0.994

(b) Proposed DLN-eCSI-D

Predicted activity

| Actual activity	Stand up	Sitting	Walk	Standing	Sit down	Running
Stand up	0.847	0.004	0.01	0.122	0.012	0.005
Sitting	0.004	0.83	0.005	0.003	0.158	0
Walk	0.003	0.003	0.965	0.011	0.001	0.017
Standing	0.031	0	0.002	0.952	0.007	0.008
Sit down	0.02	0.152	0	0.03	0.798	0
Running	0.001	0.001	0.004	0	0	0.994

(c) RNN [11]

Fig. 6. Confusion matrix for different human activity recognition methods

[10] M. Edel and E. K?ppe, "Binarized-blstm-rnn based human activity recognition," in *2016 International Conference on Indoor Positioning and Indoor Navigation (IPIN)*, Oct 2016, pp. 1–7.

[11] S. Yousefi, H. Narui, S. Dayal, S. Ermon, and S. Valaee, "A survey on behavior recognition using wifi channel state information," *IEEE Communications Magazine*, vol. 55, no. 10, pp. 98–104, OCTOBER 2017.

[12] D. Halperin, W. Hu, A. Sheth, and D. Wetherall, "Tool release: Gathering 802.11n traces with channel state information," *SIGCOMM Comput. Commun. Rev.*, vol. 41, no. 1, pp. 53–53, Jan. 2011. [Online]. Available: http://doi.acm.org/10.1145/1925861.1925870

[13] S. W. Roberts, "Control chart tests based on geometric moving averages," *Technometrics*, vol. 1, no. 3, pp. 239–250, 1959.

[14] Y. Wang, J. Liu, Y. Chen, M. Gruteser, J. Yang, and H. Liu, "E-eyes: Device-free location-oriented activity identification using fine-grained wifi signatures," in *Proceedings of the 20th Annual International Conference on Mobile Computing and Networking*, ser. MobiCom '14. New York, NY, USA: ACM, 2014, pp. 617–628. [Online]. Available: http://doi.acm.org/10.1145/2639108.2639143
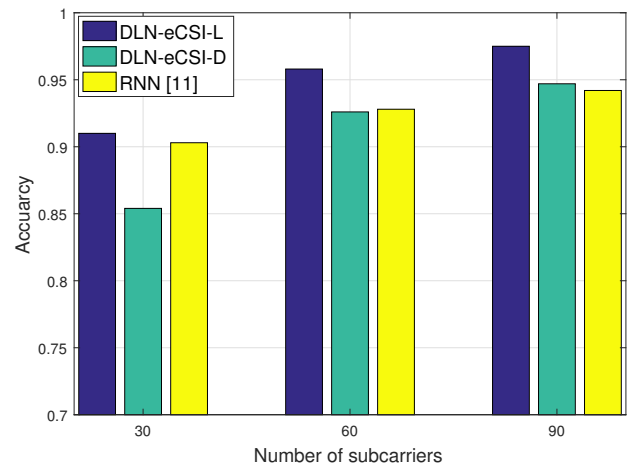
(a) The first experimental configuration
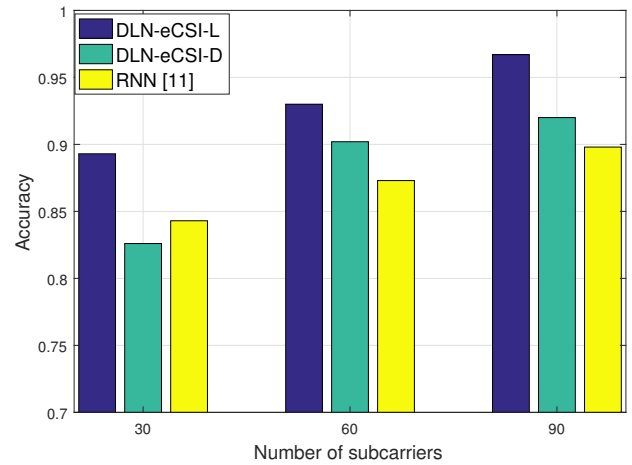
(b) The second experimental configuration

Fig. 7. Impact of the number of subcarriers on the sensing accuracy